94

CONF-9709120--

Solidification Behavior and Structure of Al-Cu Alloy Welds

J. A. Brooks, M. Li and N. C. Y. Yang
Sandia National Laboratories /CA
Livermore, CA, USA

SAND--98-8470C
RECEIVED
MAR 27 1998
OSTI

Abstract

The microsegregation behavior of electron beam (EB) and gas tungsten arc (GTA) welds of Al-Cu alloys covering a range from 0.19 to 7.74 wt% Cu were characterized for dendrite core concentrations and fraction eutectic solidification. Although a single weld speed of 12.7 mm/sec was used, some differences were observed in the segregation behavior of the two weld types. The microsegregation behavior was also modeled using a finite differences technique considering dendrite tip and eutectic undercooling and solid state diffusion. Fairly good agreement was observed between measured and calculated segregation behavior although differences between the two weld types could not be completely accounted for. The concept of dendrite tip undercooling was used to explain the formation of a single through thickness centerline grain in the higher alloy content GTA welds.

Introduction

The accurate prediction of alloy partitioning during weld solidification is desirable for many reasons. For example, to model weld solidification cracking behavior one must accurately calculate the volume fraction of liquid and solid as a function of temperature during the solidification process. The manner in which the heat of fusion is liberated during solidification also plays an important role on the shape of the solid/liquid two phase region in which the stresses or strains initiate cracks (1, 2). In many cases the solidification behavior must also be accurately described for weld microstructure evolution and properties predictions which is an important goal in the numerical modeling of welding processes (3-6).

It is known that the degree of segregation occurring during solidification is controlled by factors other than simply the phase diagram from which one can use to describe solidification using the well known Scheil equation (7). This model is an over simplification of weld solidification and other factors can contribute considerably to the final degree of microsegregation, two of the most important phenomenon being undercooling and solid state diffusion.

A number of welding studies have been conducted on the effects of undercooling and solid state diffusion in which comparisons were made between experimental results and model predictions. Brooks and Baskes (8) found that in lean Al-Cu alloys (1-2% Cu) measured dendrite tip undercooling compared reasonably well with the model of Burden and Hunt (9, 10). However, with the low alloy concentrations and solidification velocities the undercooling was only a few degrees. In modeling the solidification behavior of GTA welds in Fe-Nb alloys their finite differences analysis showed that a high degree of Nb partitioning occurs during solidification which is largely homogenized during weld solidification and cooling. Good agreement was obtained between measured microsegregation and model predictions although some uncertainty existed in alloy diffusion rates. More recently they used liquid tin quenching studies to determine the individual contributions to dendrite tip undercooling and solid state diffusion (11). At

fairly low solidification velocities, 2.1 mm/s, some dendrite tip undercooling occurred although it was negligible compared to the homogenization resulting from solid state diffusion. Again these welds were produced at fairly low velocities where the degree of undercooling is small. In this case they found a slightly better agreement with the model of Burden and Hunt (9,10) than the model of Kurz, Giovanola, and Trivedi (KGT) (12). Other studies have been conducted comparing solidification model predictions and microsegregation (4, 13-16), but relatively few studies have been conducted specifically to validate solidification model predictions in well characterized systems under commonly used welding conditions.

Materials and Experimental Procedures

Eight heats of high purity (4-9's) Al-Cu alloys were melted providing a composition range from 0.19 to 7.74 wt% Cu (all compositions are given as wt%). This system forms a simple eutectic between Al -5.65% Cu and $CuAl_2$, θ, at 821.2 K with a eutectic composition of 33.2% Cu (17). The partitioning coefficient, k, is nearly constant over the range of compositions of this study, and has a value of ~ 0.15. The alloys were solution treated and rolled into sheet material of 1.27 mm and 6.35 mm thickness for a variety of welding studies

Full penetration autogeneous GTA welds were made in the 1.27 mm sheet using welding conditions of 40 amps and 17 volts and a weld speed of 12.7 mm/s. Helium was used as the cover gas and argon was used for back side shielding. Thermocouple measurements and finite element modeling were conducted to determine the weld thermal histories. The maximum cooling rate measured at the weld centerline near the solidification front was ~ 375 K/s. Electron beam welds were produced in the 6.35 mm sheet at the same weld velocity , 12.7 mm/s, using a 6 kW Leybold Heraeus high voltage machine. The 130 kV, 20 mA electron beam was defocused 100 mA and deflected in a 3 mm circle at 1000 Hz. These parameters produced a weld depth of ~3.7 mm. Welds were made from each side of the plate to produce a full penetration weld. The maximum cooling rate in the solidification range of the EB welds, again determined from thermocouple measurements, was 975 K/s.

Dendrite core concentrations were measured along the weld centerline where it could be assumed that the solidification velocity was the same as the weld speed. Compositions were measured using an electron microprobe operated at 10 Kv and 20 nA to minimize the excited volume of material analyzed. Analytical electron microscopy was conducted on some of the EB welds to further validate the microprobe measurements. SEM image analysis techniques were used to measure the volume fraction of θ in the same region of the weld in which the core concentrations were analyzed.

Numerical Calculations

The microsegregation behavior during solidification was modeled for a cellular dendrite using a finite differences analysis with cylindrical coordinates. The numerical calculations included the effects of dendrite tip and eutectic undercooling and solid state diffusion. Dendrite tip undercooling was calculated using the model of Kurz, Giovanola, and Trivedi, KGT (12). The volume fraction solidified at the tip concentration was calculated using the lever law in a similar fashion as that used by Sarreal and Abbaschian (18). The next portion of solidification was modeled using Scheil behavior but incorporating solid state diffusion in a finite differences analysis which also allows back diffusion into the solidified tip region. In both these phases of solidification the equilibrium value of the partitioning

DISCLAIMER

coefficient, k, was used since the kinetic effects are negligible at the rather low weld velocity (14, 19). These regions of solidification are shown in figure 1a. The solidification analysis is conducted for the volume element shown in figure 1b using a finite differences computer code Diffuse-83, as reported previously by Brooks and Baskes (8). A spatial variable (r) is rescaled from a movable boundary to a fixed boundary condition in which the boundary position (ζ) is obtained from solute conservation equations. A 100 element variable mesh is used where the spacing is finer near the interface where the concentration gradient is greatest. A temperature dependent diffusivity is used in both the solid and liquid phases, except in these calculations complete mixing in the liquid was used. The analysis of eutectic undercooling was that of Jackson and Hunt (20) where ΔT is $AV^{1/2}$, here A is a constant and V is the solidification velocity in cm/s. A value of 6 $K(s/cm)^{1/2}$ was chosen for A based on the results of Sarreal and Abbaschian (18) for Al-4.9% Cu. However, it should be noted that in our analysis the material was allowed to continue to solidifying beyond the undercooled eutectic using the same solidification path and equilibrium value of k. For comparison with experiment, the calculated fraction θ used was that obtained by assuming that all the liquid remaining at the undercooled eutectic temperature solidified by the eutectic reaction. Thus any reduction in θ due to diffusion upon further cooling was ignored. The material properties used in the calculations were: k=0.15, $D_L = 3.0*10^{-5}$ (cm^2/s), and $D_s = 0.29*\exp(-15610/T)$ (cm^2/s).

Figure 2 shows the calculated concentration profiles obtained using the above model for a GTA weld of Al-1.95% Cu with a measured cell size of 5 microns, a solidification velocity of 12.7 mm/s, a cooling rate of 375K/s, and a value of k=0.15. Distance solidified has been converted from r/R to fraction solidified and is plotted versus composition. Analysis are shown for times when solidification was just completed, and after the weld has cooled to room temperature. Final solidification occurred without the formation of any eutectic and thus above the undercooled eutectic temperature. As can be seen, back diffusion modifies the concentration profiles in the solidification boundary region but as discussed later has little effect at the dendrite core. A similar plot for Scheil solidification behavior is also shown in figure 2. In this case a significant fraction of eutectic solidification occurs at the equilibrium eutectic temperature as indicated by the shaded region in the figure. The higher core concentration in the model calculation is primarily a result of dendrite tip undercooling whereas the lack of eutectic solidification is a result of both tip undercooling and solid state diffusion.

Model results obtained using the same solidification conditions as those described above are shown in figure 3 for an alloy concentration of 3.91% Cu. Again concentration profiles are plotted at the time solidification is just complete and at room temperature. In this case it is calculated that 4.69 vol.% of the material (shaded region in figure 3) solidifies as eutectic at the undercooled eutectic temperature of 814.4 K when the maximum solid solubility reaches ~ 6% Cu. Without eutectic undercooling the calculated fraction of eutectic solidification would have been ~ 7 vol.% and would have formed at the equilibrium eutectic conditions, dashed line. It can be seen in figure 3 how the concentration changes upon cooling to room temperature. Note again the core concentration at the center region is not altered as a result of further back diffusion due to the rather low diffusivity in this system and the shallow concentration gradients. However, the concentration in the boundary region where the concentration gradients are steep does change during further cooling. It should be noted that in this case the concentration profiles are not accurate due of the way solidification continues to occur along the same path disregarding the details of eutectic behavior as discussed above. For comparison with experiment, the fraction of θ calculated with the model is assumed to be that which would form by the eutectic reaction of all the

liquid remaining at the undercooled eutectic temperature. This assumption would have a tendency to overestimate the amount of eutectic since any further effect of diffuson in dissolving the eutectic constituent below the eutectic temperature is neglected.

Results

The macrostructure of the two interpenetrating EB welds is shown in figure 4 for an alloy of Al - 5.93% Cu. The EB weld macrostructure was similar for all the alloys.

The cross sections of the GTA welds were also very similar although the solidification macrostructure at the weld centerline was different. In all welds a columnar grain structure extended form near the fusion zone boundary toward the weld centerline. In the most lean alloys the columnar grains intersected along the weld centerline region with no specific grain becoming dominate. In the alloys of higher composition, 0.97% Cu and greater, the columnar grains extended from the fusion zone boundary in a similar manner as in the leaner alloys, but intersected a single through thickness centerline grain that extended the entire length of the weld. These two characteristic macrostructures are shown in figure 5 a-d.

The microstructure of the GTA weld in an alloy of 7.74% Cu is shown at higher magnification in the SEM micrograph in Figure 6. The eutectic constituent θ is clearly shown in the Cu enriched solidification boundaries. The θ morphology was similar in all welds although the volume fraction was dependent upon alloy content.

As mentioned above, since the concentration of the dendrite tip is a function of solidification velocity it is critical that the core concentration is measured at a point where the velocity is known. This can be most accurately conducted in a region of the weld where the velocity is equal to the weld speed. In the EB welds this was done in the upper portion of the second weld pass. In the GTA welds core concentrations were measured in transverse sections in the single centerline grain, or the top center region of welds with no centerline grain. Measurements of core concentration were made in at least eight different dendrites and the values of the two lowest measurements were averaged, although typically most values varied by less than 10%. The lowest values were used since if measurements are not made exactly at the core center, higher values are obtained which overestimate core concentrations.

The dendrite tip concentration calculated with the KGT model is shown in Table 1 along with the calculated dendrite core concentration of both the EB and GTA welds. Note the core concentration calculated for both processes is virtually the same. The experimentally measured values of core concentrations of both weld types are also shown in Table 1. This data is plotted in figure 7 along with the values of C_0k which would be the core concentration assuming Scheil behavior. In this case the model predictions are representative of both processes.

The calculated and experimentally measured volume fraction θ for both the EB and GTA is given in Table 2 . In this case both the measured fraction of θ is different for the two weld types, but again the calculated values are very similar. This data is plotted in figure 8 along with the volume fraction θ calculated assuming Scheil behavior and a density of α-Al of 2.82 gm/cc which is needed to calculate the fraction θ in the eutectic mixture.

Discussion

Since the dendrite tip velocity in the region measured and modeled are the same for both weld processes, the calculated concentration of the solidifying dendrite tip is also the same. These values are shown for the different compositions in Table 1. It can be seen that the calculated concentrations at the center of the dendrite cores of the EB welds are only slightly higher than the concentrations of the solidifying dendrite tip. Given the rather slow diffusion rate of Cu in Al and the cell size and cooling rate of the EB welds, back diffusion has only a small effect in changing the composition at the center of the dendrite core. It is also interesting to note that the calculated core concentrations of the EB and GTA welds are virtually the same. This is a consequence of the slower cooling rate of the GTA weld being offset by the larger diffusion distances. Using a simple $x = (Dt)^{1/2}$ analysis, it can be seen that the 3 micron cell size and 975K/s cooling rate of the EB welds are basically equivalent to the 5 micron cell size and 375K/s cooling rate of the GTA welds. Here x is the diffusion distance, D the diffusivity and t, time.

From figure 7, comparisons can be made between the measured and calculated dendrite core concentrations and the values C_0k which corresponds to the core concentrations assuming simple Scheil behavior. It can be seen that even at the fairly low solidification velocities dendrite tip concentrations are considerably higher than what is calculated neglecting tip undercooling, i.e. Scheil behavior. It can also be seen that the measured core concentrations of the GTA welds are in all cases higher than those of the EB welds. The calculated core concentrations in general lie between the measured values of the two weld types. Since the core concentrations are related primarily to tip undercooling with only a small contribution to solid state diffusion, Table 1, the experimental data shows fairly good agreement with the KGT model, especially with the EB weld data.

The calculated and measured volume fraction θ are shown in Table 2 and figure 8. Like core concentrations, there is little difference in the calculated values between the EB and GTA welds. This again is due to the compensating effects of cell sizes and cooling rates of the two weld types. It can also be seen that reasonable agreement exists between the calculated and measured values of θ content. Although considerable scatter may be expected with the image analysis measurements of the complex θ morphology, it can be seen that the measured values of the two processes are fairly close and the data is well behaved. However, like with dendrite core concentrations there are some differences between the two weld types; the measured amount of θ in the EB welds is consistently higher than that of the GTA welds. For example, in the 1.95% Cu alloy no θ was observed in the GTA welds which is consistent with model predictions, while ~0.4 % θ was observed in the EB welds. However it can be seen in figure 8 that both the measured and calculated θ contents are considerably less than what would be predicted with Scheil behavior.

Since the fraction θ is calculated at the time of solidification of the undercooled eutectic, the role of solid state diffusion on further cooling is not considered. Diffusion during further cooling would somewhat decrease the amount of the eutectic constituent, but as previously demonstrated it plays less of a role at the lower temperatures (8). However, in this regime diffusion may still play a larger role in the GTA welds than in the EB welds in reducing the θ content due to the slower cooling rate. This may account for the lower measured θ contents than those calculated, and some of the differences between the two weld types.

Still there is reasonably good agreement between the model predictions and experimental results.

One may expect from a conservation of solute standpoint that in a given alloy the higher the core concentration the smaller the fraction of eutectic solidification. The data is consistent in this manner in that the measured core concentrations of the GTA welds are higher than those of the EB welds, but the volume fraction of θ is less. Several obvious differences in the two weld types that may result in differences in solidification behavior are the thermal gradient and the solidification cell size. However, as discussed above these difference are off-setting when considering diffusional effects.

The differences in core concentration of the two processes can not be accounted for with the KGT model. An error that can be introduced in experimentally determining the dendrite core concentration is an uncertainty in dendrite velocity. Care was taken in selecting regions of the weld where the solidification velocity was close to that of the weld speed. Figure 9 shows the dendrite tip undercooling and tip concentration from the KGT model plotted against solidification velocity for two alloy compositions, 3.91 and 0.97%. The results are plotted for two different thermal gradients, an order of magnitude less and an order of magnitude greater than that of the GTA weld. The order of magnitude higher cooling rate is greater than the factor of ~3 experimentally measured in the EB welds. It can be seen that in this regime of cooling rates, tip undercooling is independent of thermal gradient; that is, the two plots overlay.

It can also be seen in figure 9 that the degree of undercooling at a given solidification velocity increases with alloy composition and that the rate of increase is higher at lower solidification velocities. In this study we have used a solidification velocity of 12.7 mm/sec. It can be seen that any error in tip velocity will have a larger effect on tip concentration for the 3.91% Cu alloy that the 0.97% Cu alloy. A error of 25% in the tip velocity results in ~±0.2 wt.% Cu variation in the composition of the dendrite tip for the 3.91% Cu alloy compared to ~±0.0 2 wt.% Cu variation for the 0.97% Cu alloy. This is considerably less than the differences in the experimentally measured core concentrations of the two weld types. As discussed above the experimental error in the microprobe should be considerably less than 10% of the measured value. Thus although there is fairly good agreement with calculated and measured core concentration and volume fraction θ, there still appears to be a difference in core concentration of the two processes that can not be accounted for by differences solely in cooling rates or dendrite orientation or experimental measurements. A further possibly from an experimental standpoint is a slight difference in solidification structure which was not detected.

Grain Orientation

The single centerline grain formation in the higher alloy content GTA welds is an interesting phenomenon that warrants more discussion. As reported elsewhere this behavior can be explained in terms of dendrite tip orientation and tip undercooling (21, 22). It has been noted that the pool solid/liquid interface is not an isotherm but changes in temperature from the fusion zone boundary to the weld centerline (21, 23). If one considers the interface velocity normal to the solidifying interface in an elliptical weld pool the velocity changes from 0 at the fusion zone boundary to the weld speed along the weld centerline. The degree of the undercooling can be seen from figure 9 showing undercooling vs solidification velocity for two different compositions. Thus the liquidus temperature at the weld centerline is less than that at the fusion zone boundary. The other factor that is important when considering the single centerline grain is the orientation of the

dendrite tip with respect to the solidification front, since it is the tip velocity that determines the degree of undercooling. This is shown schematically in figure 10 for two grains intersecting near the weld centerline similar to that observed in the welds with the single centerline grains in figure 5. The grain structure in this region has evolved through a competitive growth process beginning at the fusion zone boundary. The velocity component normal to the solid liquid interface is closely aligned with the maximum thermal gradient and can be defined as $V_N = V_W \cos\psi$ (in a thin sheet, or two dimensional weld) where V_W is the weld velocity and ψ is defined in figure 10. It can be seen geometrically in figure 10 that the velocity of the dendrite tips, V_t of the intersecting grain will be higher than those of the centerline grain and is given as $V_t = V_w \cos\psi / \cos(\phi - \psi)$ as defined in the figure. Thus the centerline grain will be solidifying at a lower velocity and higher temperature (less undercooling) than the adjacent columnar grains. As a consequence the centerline grain will be growing ahead of the intersecting grains and can continue to grow until the welding process or thermal conditions are interrupted . Direct evidence of this growth behavior has been reported by Li and Brooks (22) in GTA welds in Ti-6Al-4V.

In this analysis it is suggested that the centerline grain is stabilized by the fact that it is growing at a higher temperature than the adjacent grains. In figure 9 it can be seen that at the solidification velocity of 12.7 mm/sec, changes in growth rate result in larger changes in undercooling in higher than in lower alloy compositions. With the welding parameters used in this study, the centerline grain was observed in the GTA welds of all alloys of 0.97% Cu and greater, but in no alloys of 0.49% Cu and less. From figure 10 it appears that only a small difference in undercooling is sufficient to stabilize the centerline grain under the welding conditions and geometries used in this study. It should be noted that the welds in this study and in Ti-6Al-4V (22), were full penetration with near vertical fusion zone boundaries.

Summary

Microsegregation was modeled using a finite differences analysis that included dendrite tip and eutectic undercooling and solid state diffusion. Model predictions were compared with experimental analysis of EB and GTA welds made on a series of eight Al- Cu alloys. The alloys covered a composition range from 0.19 to 7.74 % Cu. Comparisons were made between the measured and predicted dendrite core concentration and the fraction of eutectic constituent θ. It was found that even at the moderate welding speeds of 12.7 mm/s that considerable undercooling occurs. The measured core concentrations of the GTA welds were somewhat higher than those of the EB welds for all alloy compositions. However, fairly good agreement was obtained between the model prediction and measured core concentrations with the predictions falling between the measured values of the two processes. Under the conditions of welding, the calculated concentrations at the core center were virtually unchanged from that calculated using the KGT theory of tip undercooling. This is due to the limited back diffusion into the tip region resulting from the rather low diffusivity of Cu in Al. The differences is core concentration between the two processes could not be accounted for in the model.

Fairly good agreement was also observed between the calculated fraction of θ and that formed during the undercooled eutectic reaction and that experimentally measured. Experimentally it was found that the measured fraction θ was slightly higher in the EB welds than the GTA welds of the same alloy composition. In both cases the fraction was considerably less than the value predicted assuming Scheil behavior. The model predictions for both the core concentrations and fraction θ were very similar for both weld processes.

This is a consequence of the same solidification velocity of both processes and the off-setting effects of cell sizes and cooling rates resulting in very similar solid state diffusion behavior.

A single centerline grain that formed in the higher alloy content GTA welds was explained in terms of dendrite tip undercooling and dendrite orientation. It is proposed for welds with a single through thickness centerline grain that the dendrites in the centerline grain grow at a lower velocity and higher temperature (less undercooling) than the impinging adjacent grains.

Acknowledgments

The authors would like to thank J. Krafcik and A. Gardea of Sandia National Laboratories for conducting weld experiments and for metallographic support. This work is supported by the U.S. Department of Energy under contract No. DE-AC04-94AL 85000 and the U. S. Department of Energy, Office of Basic Energy Science.

Figure Captions

Figure 1. (a) Solidification behavior showing three regions modeled including: I, tip undercooling; II, modified Scheil behavior, and III, eutectic undercooling where C_m is the equilibrium maximum solid solubility of Cu in Al and C_E is the undercooled eutectic composition (b) volume element for which solidification was modeled showing nature of variable mesh.

Figure 2. Compositional profils calculated for a GTA weld of Al-1.95% Cu after solidification is completed (without eutectic solidification) and after cooling to room temperature. Scheil behavior is shown for comparison where the dashed lines correspond to the region of eutectic solidification.

Figure 3. Compositional profile calculated for a GTA weld of Al-3.91% Cu at point of undercooled eutectic solidification and after cooling to room temperature. Dashed line corresponds to the fraction eutectic without eutectic undercooling

Figure 4. Macrostructure of EB welds in alloy of Al-5.93% Cu.

Figure 5. Microstructure of GTA welds (a) longitudinal and (b) transverse section in Al-0.19% Cu alloy; (c) longitudinal and (d) transverse section in Al- 3.91% Cu.

Figure 6. SEM micrograph of GTA weld in Al-7.74% Cu showing eutectic θ at the solidification cell boundaries.

Figure 7. Calculated and measured core concentrations of the two weld types for all alloy compositions. Calculated results are the same for both processes. The value of C_0k (k=0.15) for Scheil behavior is shown for comparison.

Figure 8 Calculated and measured $CuAl_2$, θ , content of the two weld types for all compositions. Results for Scheil behavior is shown for comparison.

Figure 9. Dendrite tip concentration and undercooling vs tip velocity for two alloy concentrations. Values are nearly the same for the two different thermal gradients.

Figure 10. Schematic of intersecting grains along weld centerline showing higher tip velocity in impinging grain than in centerline grain.

References

1.Feng, Z. and Tsai, C. L., "Modeling the Thermomechanical Conditions at Weld Pool", Proc. Modeling and Control of Joining Processes, ed. T. Zacharia, AWS, 1993, p. 533-540.

2.Dike, J. J., Brooks, J. A., and Krafcik, J. S., "Finite Element Modeling and Verification of Thermal-Mechanical Behavior in the Weld Pool Region", Proc. 4th International Conference on Trends in Welding Research, ed. H. B. Smartt, J. A. Johnson, and S. A. David, ASM International, 1995, p. 159-164.

3. Olsen, G., " Influence of Post Weld Heat Treatment", this proceedings.

4. Matsuda, F., Nakagawa, H. and LEE, J., Quart. J. Japan Welding Soc., 1991, vol. 9(1), p. 85-92.

5. Brooks, J.A. and Gardea, A.D., "Weld Microsegregation and Microstructural Evolution of Several Stainless Steel Alloys", Microstructural Science vol .20, Metallographic Characterization of Metals after Welding, Processing and Service, Conf. Proc. ASM Inter. and Inter. Metallographic Soc., ed. Kanne, Johnson, Braun, and Louthan, ASM International, 1993, p. 3-15.

6. Vitek, J. M., "Modeling the Ferrite-Austenite Transformation in Stainless Steel Welds,: Results, Comparison with Experiment, and Potential Applications", this proceedings.

7. Scheil, E., Z. Metallkunde, vol. 34, 1942, p. 70-72.

8. Brooks, J. A. and Baskes, M. I., "Weld Microsegregation Characterization and Modeling", Inter. Conf. on Trends in Welding Research, ed. S. David, ASM International, 1986, p. 93-99.

9. Burden, M. H. and Hunt, J. D., "Cellular and dendritic growth I", Journal of Crystal Growth, vol. 22, 1974, p. 99-108.

10. Burden, M. H. and Hunt, J. D., "Cellular and dendritic growth II", Journal of Crystal Growth, vol. 22, 1974, p. 109-116.

11. Brooks, J. A., Li, M., Baskes, M. I., and Yang, N. Y. C., "Roles of dendrite tip undercooling and solid state diffusion on weld microsegregation of Fe-Nb welds", accepted for publication in Science and Technology of Welding and Joining, 1997.

12. Kurz, W., Giovanola, B., and Trivedi, R., "Theory of microstructural development during rapid solidification", Acta Metallurgica, vol. 34, 1986, p. 823-830.

13. Elmer, J. W., "The influence of cooling rate on the microstructure of stainless steel alloys", Ph.D. Thesis, MIT, 1988.

14. Elmer, J. W., "Non-equilibrium solidification in austenitic stainless steel welds", The Metal Science of Joining, ed. M. J. Cieslak, J. H. Perepezko, S. Kang, and M. E. Glicksman, ASM International, 1992, p. 115-133.

15. Brooks, J. A., Baskes, M. I., and Greulich, F. A., "Solidification modeling and solid state transformations in high energy density welds", Metall. Trans. A., vol. 22A, 1991, p. 915-925.

16. Boettinger, W. J., Bendersky, L. A., Coriell, S. R., Schaefer, R. J., Biancaniello, F. S., "Microsegregation in rapidly solidified Ag-15wt.% Cu alloys", Journal of Crystal Growth, 1987, vol. 80(#1), p. 17-25.

17. Massalski, T. B., Binary Alloy Phase Diagram, Second Edition. ASM International, 1990, p. 226 and 3495.

18. Sarreal, J. A. and Abbaschian, G. J., "The effects of solidification rate on microsegregation", Metallurgical Transactions A, vol. 17A(11), 1986, p. 2063-2073.

19. Trivedi, R. and Kurz, W., "Dendritic growth", International Materials Reviews, vol. 39(2), 1994, p. 49-74.

20. Jackson, K. A. and Hunt, J. A., "Lamellar and rod growth", Trans AIME, 1966, vol. 236, p. 1129-1142.

21. Brooks, J. A., "Keynote address: weld solidification and microstructure development", Proceeding of 4th International Conference on Trends in Welding Research, ed. H. B. Smartt, J. A. Johnson, and S. A. David, ASM International, 1996. p. 123-134.

22. Li, M. and Brooks, J. A., "Mechanism of Single Centerline Grain Formation in Titanium Alloy Welds", accepted for publication in Science and Technology of Welding and Joining, 1997.

23. Kurz, W. and Trivedi, R., "Keynote address: modern solidification theory applied to welding", Proceeding of 4th International Conference on Trends in Welding Research, ed. H. B. Smartt, J. A. Johnson, and S. A. David, ASM International, 1996, p. 115-120.

Table 1. Dendrite core concentrations for different alloy compositions, % Cu.

Alloy Compositions (Cu, wt. %)	0.19	0.49	0.97	1.95	2.97	3.91	5.93	7.74
C_{tip} (Cu, wt. %)	0.10	0.21	0.36	0.63	0.90	1.13	1.61	2.02
Model - EB (Cu, wt. %)	0.12	0.24	0.40	0.69	0.97	1.21	1.71	2.14
Model - GTA (Cu, wt. %)	0.11	0.23	0.40	0.69	0.97	1.21	1.71	2.14
Experiment - EB (Cu, wt. %)	0.11	0.17	0.32	0.79	0.91	1.15	1.51	1.82
Experiment - GTA (Cu, wt. %)	0.07	0.44	0.64		1.55	1.68	1.89	2.51

Table 2. Volume fraction $CuAl_2$ for different alloy compositions

Compositions (Cu, wt. %)	0.19	0.49	0.97	1.95	2.97	3.91	5.93	7.74
Model - EB ($CuAl_2$, vol. %)	0.00	0.00	0.00	0.00	1.04	2.07	4.36	6.50
Model - GTA ($CuAl_2$, vol. %)	0.00	0.00	0.00	0.00	1.08	2.11	4.39	6.52
Experiment - EB ($CuAl_2$, vol. %)	0.00	0.12	0.21	0.48	0.81	1.48	3.50	5.99
Experiment - GTA ($CuAl_2$, vol. %)	0.00	0.00	0.00	0.00	0.38	0.90	3.33	5.46

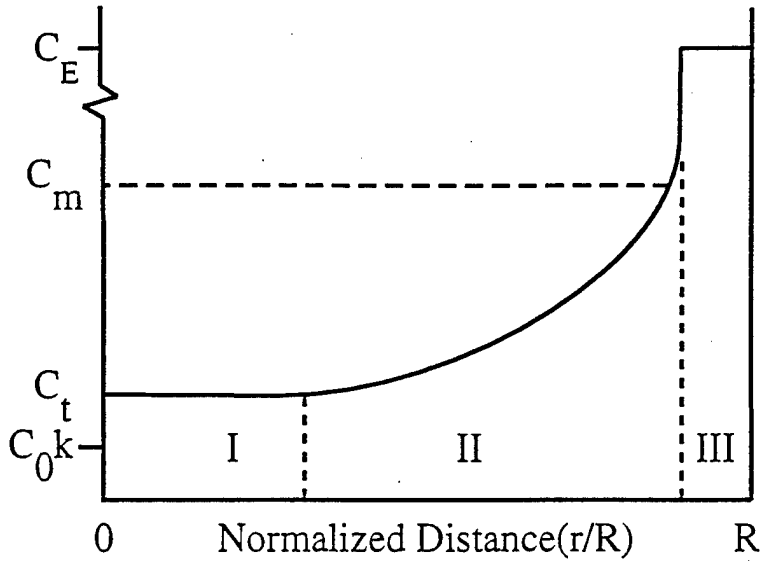
C_E
C_m
C_t
C_0k
I
II
III
0
Normalized Distance(r/R)
R

a

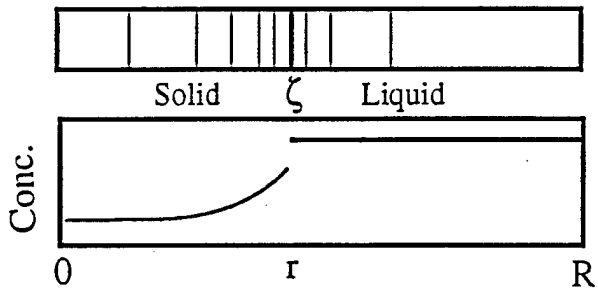
Solid
ζ
Liquid
Conc.
0
r
R

b

Figure 1

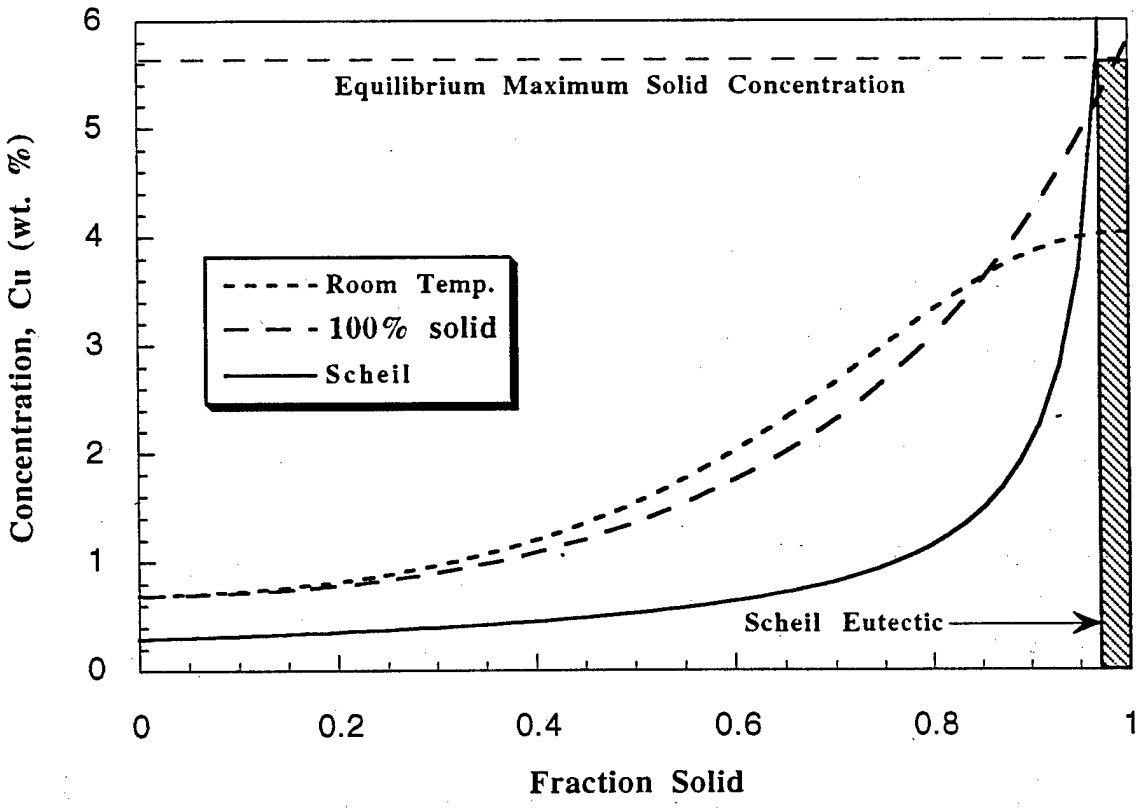
Equilibrium Maximum Solid Concentration
Room Temp.
100% solid
Scheil
Scheil Eutectic
Concentration, Cu (wt. %)
Fraction Solid
0
1
2
3
4
5
6
0
0.2
0.4
0.6
0.8
1

Fig 2

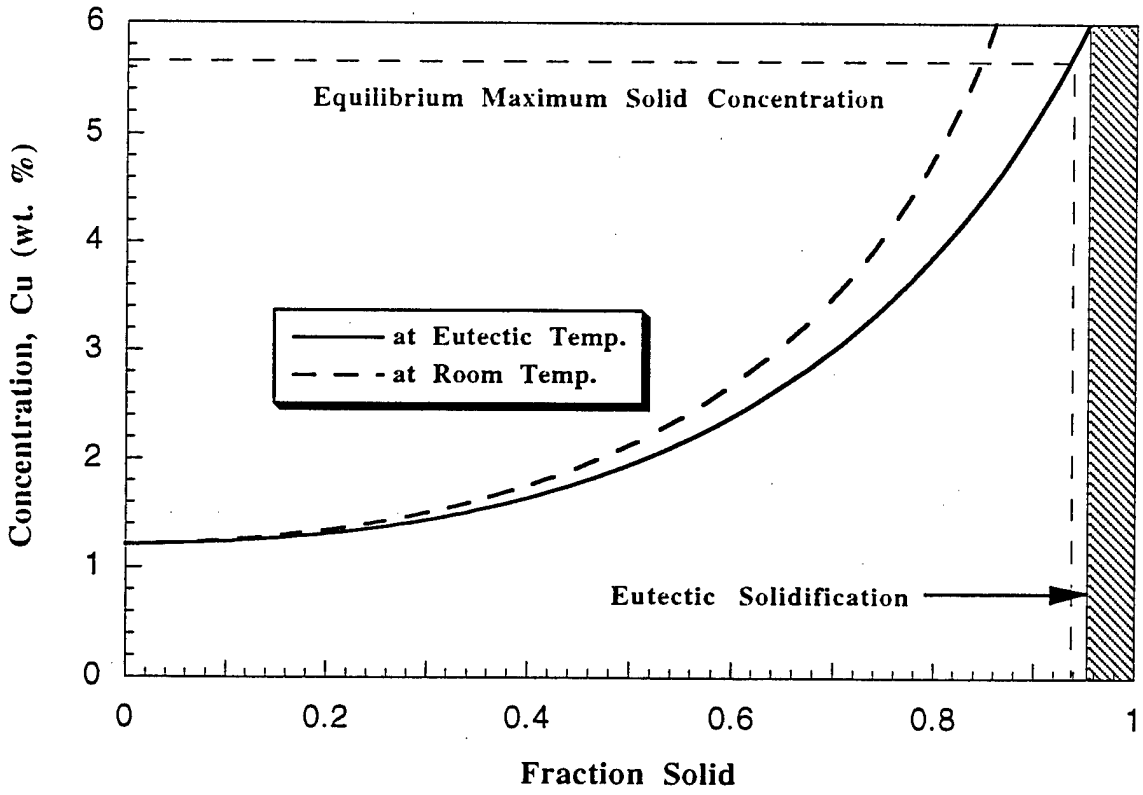
Concentration, Cu (wt. %)
6
5
4
3
2
1
0
Equilibrium Maximum Solid Concentration
at Eutectic Temp.
at Room Temp.
Eutectic Solidification
0
0.2
0.4
0.6
0.8
1
Fraction Solid

Fig 3

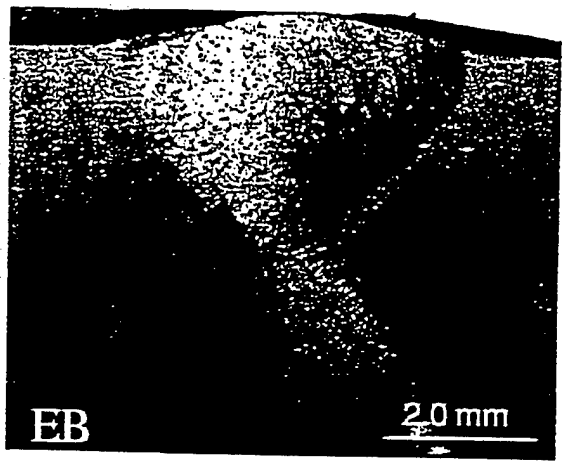

Fig 4

Figure 5

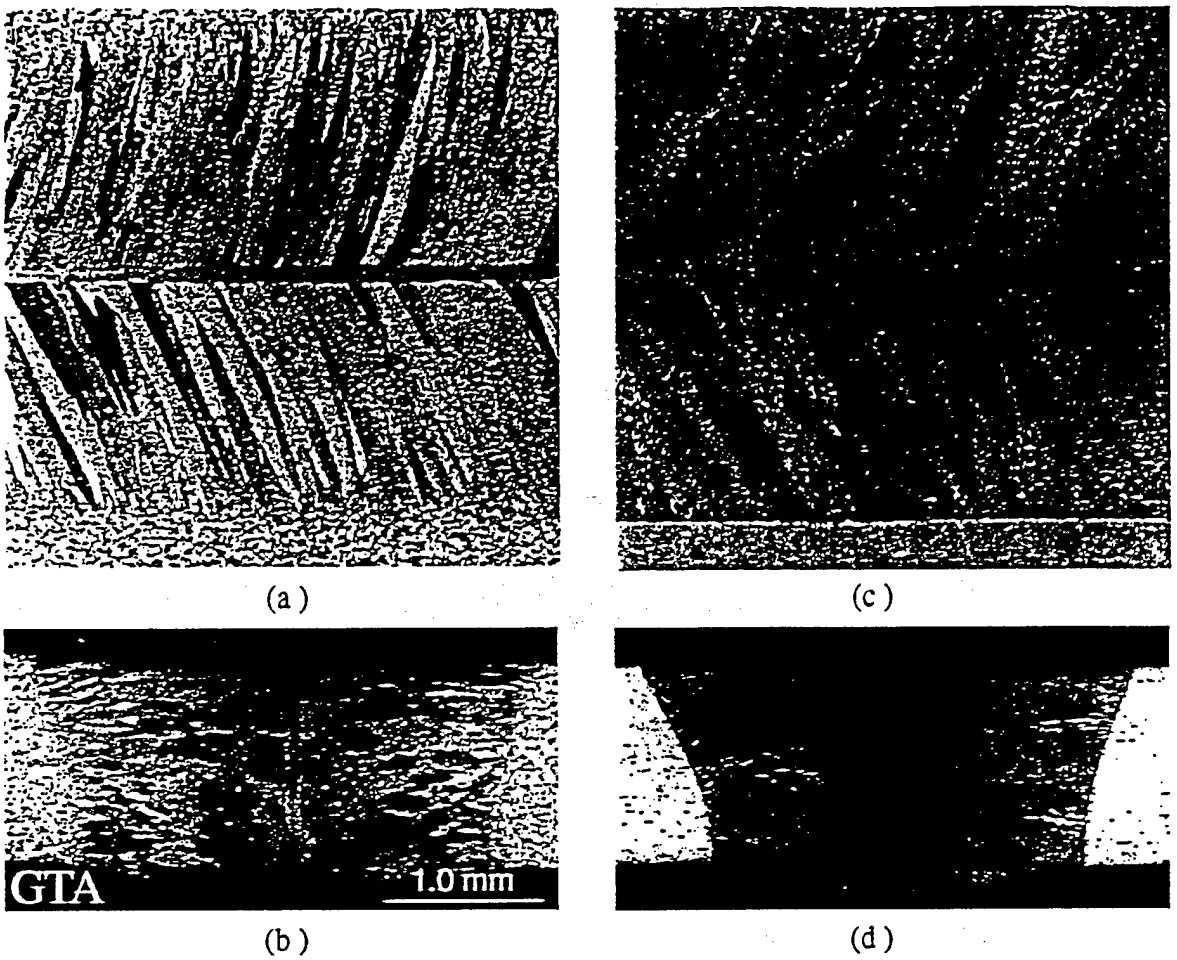

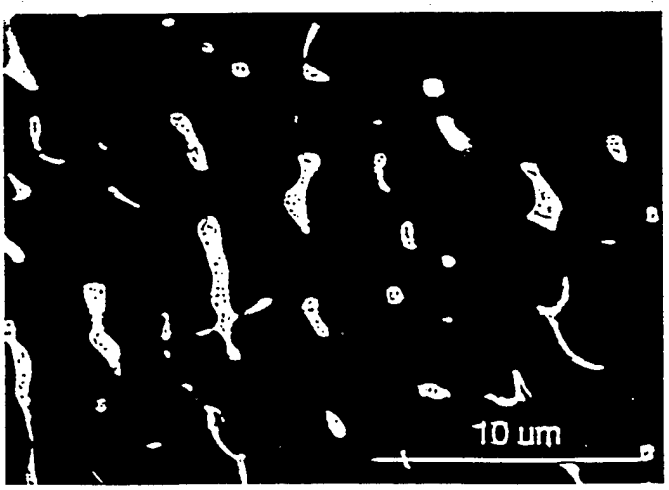

Fig 6

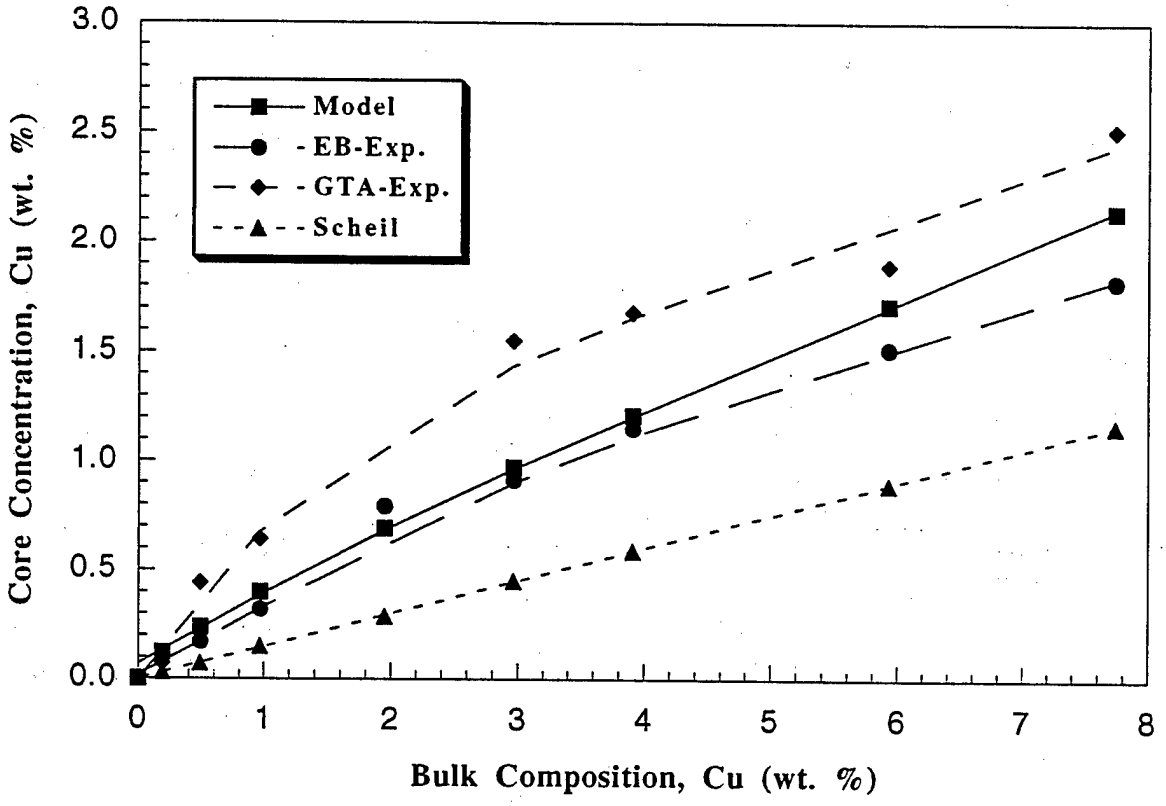
Model
- EB-Exp.
- GTA-Exp.
- - Scheil
Core Concentration, Cu (wt. %)
Bulk Composition, Cu (wt. %)
0.0
0.5
1.0
1.5
2.0
2.5
3.0
0
1
2
3
4
5
6
7
8

Fig 7

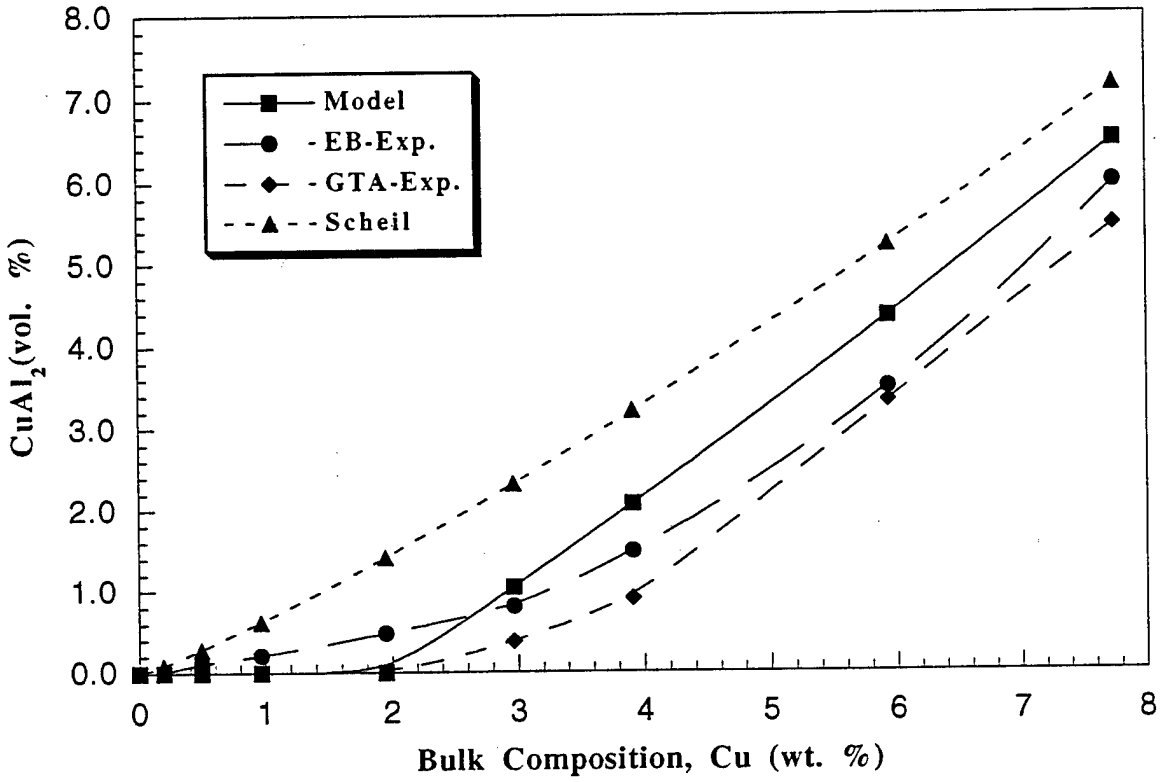
8.0
7.0
6.0
5.0
4.0
3.0
2.0
1.0
0.0
0
1
2
3
4
5
6
7
8
Model
- EB-Exp.
- GTA-Exp.
Scheil
CuAl2(vol. %)
Bulk Composition, Cu (wt. %)

Fig 2

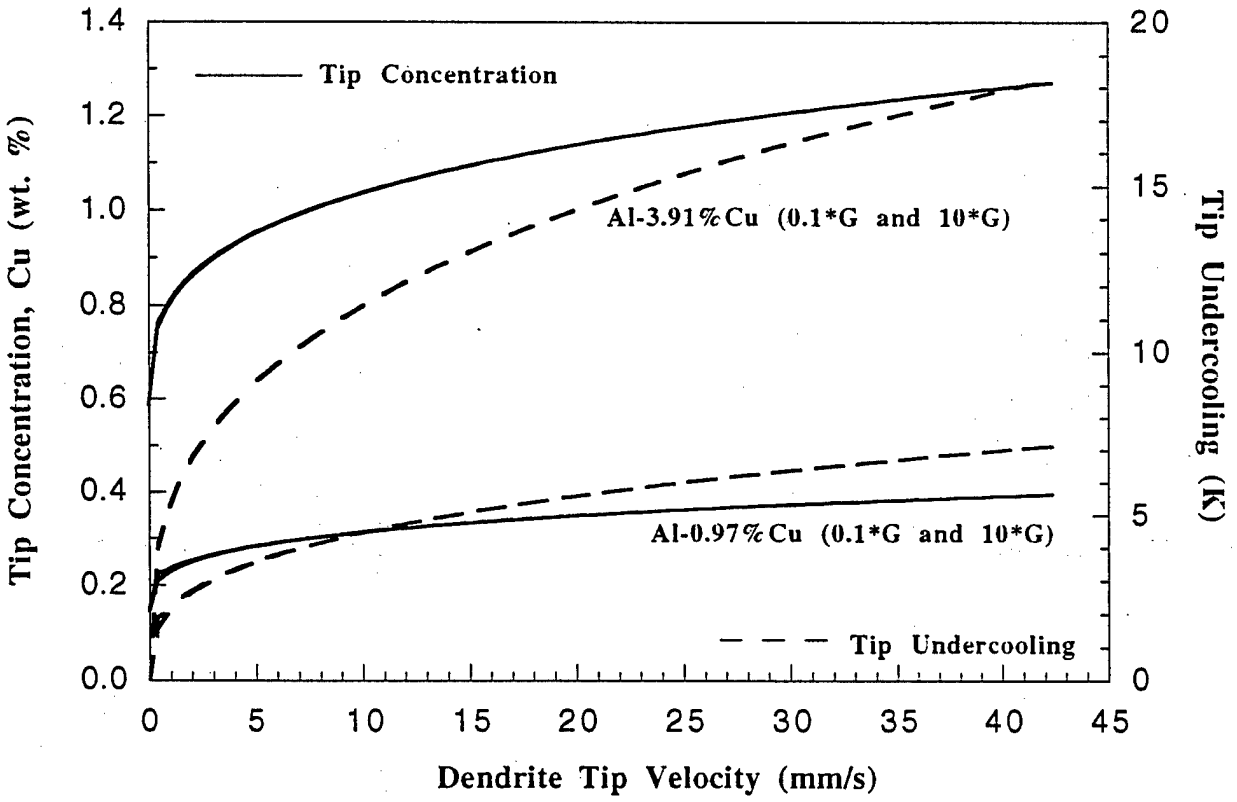
Tip Concentration
Al-3.91%Cu (0.1*G and 10*G)
Al-0.97%Cu (0.1*G and 10*G)
Tip Undercooling
Tip Concentration, Cu (wt. %)
Tip Undercooling (K)
Dendrite Tip Velocity (mm/s)
1.4
1.2
1.0
0.8
0.6
0.4
0.2
0.0
20
15
10
5
0
0
5
10
15
20
25
30
35
40
45

Fig 9

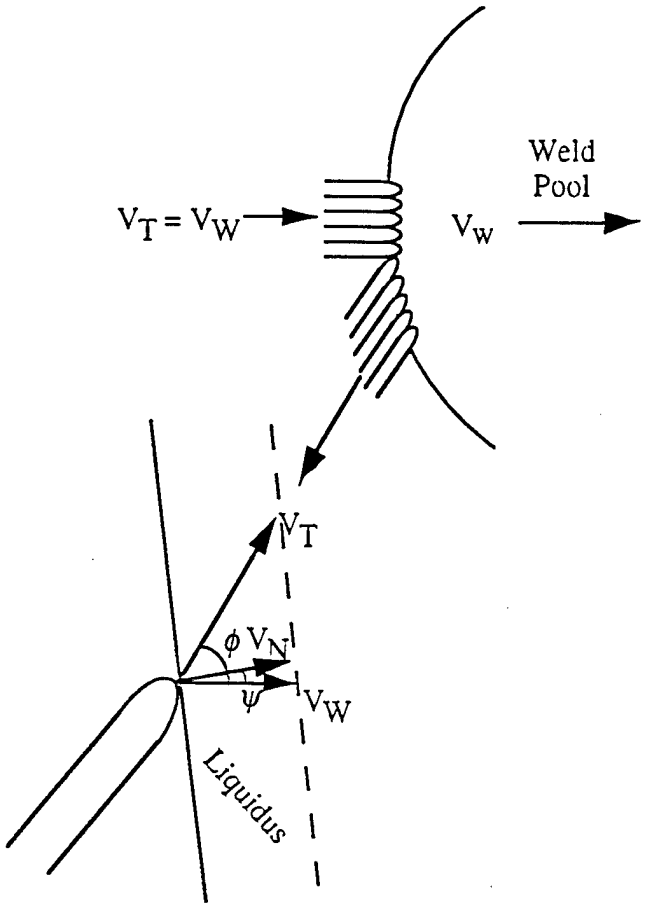

Fig 10

Report Number (14) SAND--98-8470C
CONF-970912--

Publ. Date (11) 199709
Sponsor Code (18) DOE/ER, XF
UC Category (19) UC-404, DOE/ER